A Theory of Deep Stratification and Overturning Circulation in the Ocean

MAXIM NIKURASHIN AND GEOFFREY VALLIS

Princeton University, Princeton, New Jersey

(Manuscript received 1 July 2010, in final form 29 October 2010)

ABSTRACT

A simple theoretical model of the deep stratification and meridional overturning circulation in an idealized single-basin ocean with a circumpolar channel is presented. The theory includes the effects of wind, eddies, and diapycnal mixing; predicts the deep stratification in terms of the surface forcing and other problem parameters; makes no assumption of zero residual circulation; and consistently accounts for the interaction between the circumpolar channel and the rest of the ocean.

The theory shows that dynamics of the overturning circulation can be characterized by two limiting regimes, corresponding to weak and strong diapycnal mixing. The transition between the two regimes is described by a nondimensional number characterizing the strength of the diffusion-driven compared to the wind-driven overturning circulation. In the limit of weak diapycnal mixing, deep stratification throughout the ocean is produced by the effects of wind and eddies in a circumpolar channel and maintained even in the limit of vanishing diapycnal diffusivity and in a flat-bottomed ocean. The overturning circulation across the deep stratification is driven by the diapycnal mixing in the basin away from the channel but is sensitive, through changes in stratification, to the wind and eddies in the channel. In the limit of strong diapycnal mixing, deep stratification is primarily set by eddies in the channel and diapycnal mixing in the basin away from the channel, with the wind over the circumpolar channel playing a secondary role. Analytical solutions for the deep stratification and overturning circulation in the limit of weak diapycnal mixing and numerical solutions that span the regimes of weak to strong diapycnal mixing are presented.

The theory is tested with a coarse-resolution ocean general circulation model configured in an idealized geometry. A series of experiments performed to examine the sensitivity of the deep stratification and the overturning circulation to variations in wind stress and diapycnal mixing compare well with predictions from the theory.

1. Introduction

This paper tries to make progress in the problem of understanding the deep stratification and associated overturning circulation in the ocean. In addition to being a fundamental aspect of the Earth's ocean the deep structure is of direct importance to the climate system; however, compared to some other aspects of the large-scale ocean circulation, it has been inadequately studied and is rather poorly understood. Here, we present a simple theoretical model (or theory, for short) of this structure; the theory is not complete and focuses on the zonally averaged circulation and stratification, but it makes specific predictions and we also describe some tests of these predictions with a numerical model.

The ocean's stratification is concentrated in the upper several hundred meters, where it gives rise to the seasonal and main thermocline, and, not surprisingly, most of the research efforts in both observing and understanding the stratification have been concentrated there, stemming at least in part from Robinson and Stommel (1959) and Welander (1959), who proposed diffusive and adiabatic theories, respectively, and continued apace over the following decades (e.g., Stommel and Webster 1963; Welander 1971; Colin de Verdière 1989). Development of the adiabatic theory led to the well-known ventilated thermocline model of Luyten et al. (1983), extended by Killworth (1987) and Huang (1988); a diffusive counterpart was proposed by Salmon (1990), and a model in which the upper thermocline is adiabatic but has a diffusive base was finally suggested by Samelson and Vallis (1997). Although some aspects of the stratification of the upper ocean remain rather poorly understood—for example, the role of mesoscale eddies as well as the

Corresponding author address: Maxim Nikurashin, AOS Program, Princeton University, Princeton, NJ 08540.
E-mail: man@alum.mit.edu

DOI: 10.1175/2010JPO4529.1

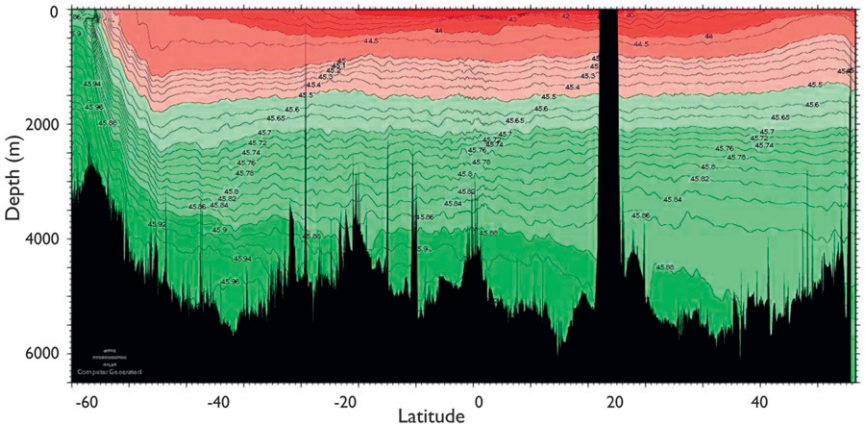

FIG. 1. Meridional section of potential density σ_4 (kg m^{-3}) in Pacific Ocean at approximately 150°W from World Ocean Circulation Experiment (WOCE) P16.

determination of the thermocline depth on the eastern boundary in the theory of the ventilated thermocline—our understanding might be said to be in a reasonably mature state.

The same cannot be said for the middepth and abyssal circulation, which we henceforth simply refer to as the deep circulation, and associated stratification. Observations show the presence of small but nonnegligible stratification below the main thermocline (Fig. 1), and it is this structure we seek to understand.

Over the years, a number of mechanisms have been proposed for the maintenance of the deep circulation of the ocean. One early model was that of Stommel and Arons (1960); this work became something of a paradigm and subsequent ideas were for a long time based on it. The model is successful in predicting a deep western boundary current but fails in a number of other ways. Most relevant to this study, the model does not address the origin of the observed deep stratification except in so far as it is implicitly predicated on an advective–diffusive balance over much of the ocean, an issue that was discussed by Pedlosky (1992). Of course, if there is sufficient diapycnal mixing, then a deep stratification is to be expected and can be maintained by an advective–diffusive balance, as was essentially posited by Munk (1966) and Munk and Wunsch (1998) and utilized in the theory of Pedlosky (1992). A large diapycnal diffusivity essentially serves to pull stratification downward from the main thermocline into the abyss, but it seems that an unrealistically large diffusivity would be required for this process alone to maintain the observed deep stratification shown in Fig. 1 and the observed rate of overturning circulation. Consistently, numerical models in closed basins produce very little deep stratification if diapycnal mixing is realistically small (Salmon 1990; Samelson and Vallis 1997): the abyss simply fills up with the densest available water, leading to an unstratified abyss, and simply having a larger abyssal diffusivity does little to create abyssal stratification. This picture is not significantly altered by the presence of mesoscale eddies (Henning and Vallis 2004). The eddies do modify the structure of the main thermocline but are unable by themselves to provide significant deep stratification.

An interhemispheric overturning circulation of a rather different nature than the Stommel–Arons picture seems to have been envisioned by Eady (1957); independently proposed by Toggweiler and Samuels (1998); and extended and further modeled by Gnanadesikan (1999), Vallis (2000), Samelson (2004, 2009), and Wolfe and Cessi (2010). This circulation relies on the mechanical forcing within the Southern Ocean in conjunction with a density difference between the surface waters in the North Atlantic and the edge of the circumpolar channel. If the North Atlantic surface is sufficiently dense and the diffusivity sufficiently low then North Atlantic Deep Water (NADW) will not necessarily upwell diffusively in the subtropics through the main thermocline but will cross into the Southern Hemisphere and upwell in the Southern Ocean. There is both observational and numerical support for such a picture, but it does not address the origin of the observed deep stratification in the ocean except in so far as it may be maintained by NADW overlaying the abyssal Antarctic Bottom Water (AABW). This is not to say that aspects of the abyssal circulation have not been studied theoretically. Kamenkovich and Goodman (2000), for example, studied the dependence of the volume and transport of the AABW on vertical diffusivity using both an idealized numerical model and various theoretical scalings, although without taking into account the effects of geometry and mesoscale eddies in the Southern Ocean. Taking a different perspective, Ito and Marshall (2008) suggested that eddies in the circumpolar channel

play a crucial role in the dynamics of the lower cell of the overturning circulation in the Southern Ocean. The authors suggested a scaling for the transport of the AABW within the latitude band of the circumpolar channel based on a balance between the isopycnal advection of buoyancy by a combination of the wind-driven and eddy-induced circulation and the cross-isopycnal diffusion by enhanced diapycnal mixing. Both of the above two studies suggest that the lower cell of the overturning circulation is intrinsically diabatic.

Our own approach to the problem is motivated both by these studies and by a number of recent numerical simulations that suggest that deep stratification can be produced if a reentrant channel in the Southern Ocean is present. Such stratification arises even with no eddies if topography is present (Vallis 2000) and even with no topography if eddies are present (Henning and Vallis 2005; Zhao and Vallis 2008; Wolfe and Cessi 2010). These results suggest that the deep stratification is fundamentally related to the geometry of the ocean basins and that it is much influenced and perhaps even produced by the dynamics of the Southern Ocean. There are two other notable aspects to the deep stratification as produced by the numerical simulations: the stratification arises throughout the ocean, even in the Northern Hemisphere, and the stratification appears to be maintained even as the diapycnal diffusivity tends to zero. That is, it appears that diapycnal mixing is not necessary to maintain a deep stratification, although we shall see later that it may be necessary to maintain a deep circulation.

In the rest of the paper we present a theory (by which we mean a conceptual model that makes testable predictions) for the deep stratification and the overturning circulation both in the circumpolar channel and in the basin north of the channel, which is based on the momentum and buoyancy balances and includes the effects of wind, eddies, and diapycnal mixing. The theory builds on previous work in a number of ways. It relies on a residual-mean framework (Marshall and Radko 2003, 2006; Radko 2005), matches the circumpolar channel to the ocean basin north of it (Gnanadesikan 1999; Samelson 1999), closes the circulation through the diapycnal upwelling in the ocean interior (Ito and Marshall 2008), and builds on the phenomenological understanding gained with previous numerical studies (e.g., Vallis 2000; Henning and Vallis 2005; Wolfe and Cessi 2010). The theory extends the previous work in the following ways: the theory explicitly predicts the form of the deep stratification in terms of the surface forcing and other problem parameters; it consistently accounts for the interaction between the circumpolar channel and the rest of the ocean; and it makes no assumption of zero residual circulation in the channel, even when the flow there is adiabatic. The theory does not explicitly deal with the middepth, interhemispheric circulation.

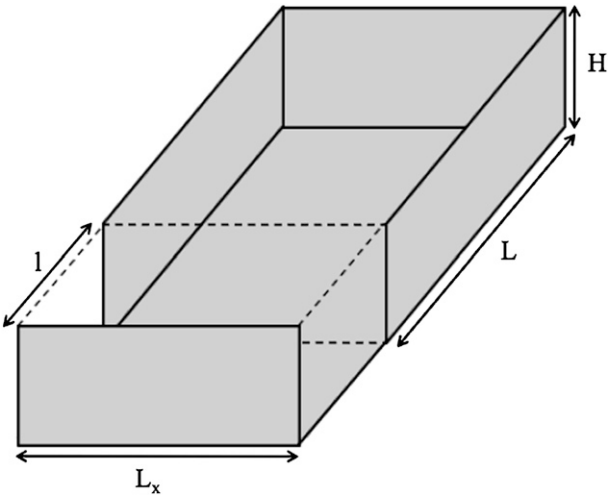

FIG. 2. Schematic of the domain. The domain consists of a rectangular basin that connects to a circumpolar full-depth channel at its southern boundary.

The paper is structured as follows: In section 2, we develop a theory for the deep stratification and overturning circulation and discuss the dependence of characteristic scales on parameters of the problem in limits of weak and strong diapycnal mixing. This is followed in section 3 by the analytical solution obtained in the limit of weak diapycnal mixing. Section 4 describes the numerical solution of the theoretical equation for a wide range of parameters. Theoretical scaling is tested with a numerical ocean general circulation model in section 5. Finally, section 6 offers discussion and conclusions.

2. Theory

a. The physical picture

Our theory is for the zonally averaged stratification and circulation of the ocean below the main thermocline and below any North Atlantic Deep Water that may be formed in the Northern Hemisphere. Specifically, we consider an ocean consisting of a closed basin (which may extend across the equator) connected to a circumpolar channel, as illustrated in Fig. 2. We take the circumpolar channel to be in the south, and we assume that the surface boundary conditions at the northern edge of the domain are such that no deep water forms in the Northern Hemisphere. We assume that an eastward wind blows over the southern channel, providing a surface stress $\tau_w(y)$, and that the surface buoyancy conditions are such that the densest surface water occurs at the southern edge of the domain and that surface buoyancy increases monotonically

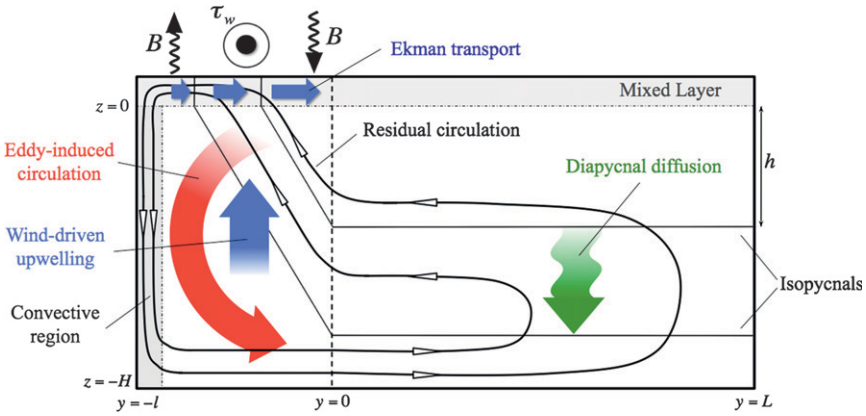

FIG. 3. Schematic of the meridional overturning circulation. Thin black lines are the isopycnals, the thick black lines with arrows are the overturning streamlines, the dashed vertical line is the northern edge of the channel, and the shaded gray areas are the convective region and the surface mixed layer.

equatorward, specified by a surface boundary condition $b_0(y)$. Roughly speaking, dense water sinks at the poleward end of the channel and moves equatorward, as illustrated in Fig. 3, potentially passing from the channel into the basin. If there is nonzero diffusivity in the basin, it may cross isopycnals before returning to the channel where it flows along isopycnals to the surface. The isopycnals in the channel are sloping, with a dominant balance between the steepening effects of the wind and the slumping effect of mesoscale eddies, and it is this slope that determines the deep stratification throughout the ocean. (Aside from mesoscale eddies, we do not explicitly account for the effects of other zonally asymmetric effects in the channel such as standing waves caused by topography or geographic effects.) The theory relies on a matching of nearly adiabatic dynamics in the circumpolar channel to the diabatic dynamics in the basin north of the channel so that there is a mutual influence between the channel and the closed basin. The rest of this section quantifies and describes in more detail this picture.

Consider first the basin north of the channel. Here, the deep isopycnals, away from the wind-driven surface-intensified circulation, are taken to be flat, which is consistent with observations and with a thermal wind balance with no zonally averaged zonal shear. In a steady state, upward advection of buoyancy by the overturning circulation is balanced by the downward diffusion. At the boundary between the basin and the channel, both the buoyancy and the overturning circulation in the basin are required to match those in the channel. In the channel, where meridional boundaries are absent, the wind-driven circulation extends through entire water column and acts to steepen isopycnals. Mesoscale eddies generated through baroclinic instability of the zonal flow cause the isopycnals to slump and drive an eddy-induced circulation that, when added to the Eulerian wind-driven circulation, forms a residual circulation. If the flow in the channel is nearly adiabatic, as we argue below that it is, then the residual circulation will be along isopycnals but not necessarily zero. The slope of the isopycnals in a statistical equilibrium is then determined by a balance between the slumping effects of the mesoscale eddies and the steepening effects of the wind-driven Eulerian circulation. The deep stratification in the basin is then influenced by the presence of mesoscale eddies in the channel, as seen in the simulations of Henning and Vallis (2005) and analyzed in more detail by Wolfe and Cessi (2010). However, as described below, a self-consistent picture also allows the dynamics in the basin to influence the stratification and overturning circulation in the channel.

b. Equations of motion

To be more specific, let us consider a single-basin rectangular domain of a uniform depth H and a full-depth channel of width l at its southern boundary (Fig. 3). We choose to couch the theory in the transformed Eulerian-mean (TEM) framework (Andrews and McIntyre 1976), a natural framework for the inclusion of eddy effects, in which the steady-state zonally averaged momentum, continuity, and buoyancy equations can be written as

$$-f\upsilon^{\dagger} = -\frac{\Delta p}{L_x} + \partial_z \tau + f\partial_z\left(\frac{\overline{\upsilon' b'}}{\partial_z \overline{b}}\right), \tag{2.1}$$

$$f\partial_z \overline{u} = -\partial_y \overline{b}, \tag{2.2}$$

$$\partial_y \upsilon^{\dagger} + \partial_z w^{\dagger} = 0, \quad \text{and} \tag{2.3}$$

$$\upsilon^{\dagger}\partial_y \overline{b} + w^{\dagger}\partial_z \overline{b} = \kappa_{\upsilon}\partial_{zz}\overline{b}, \tag{2.4}$$

where $v^\dagger$ and $w^\dagger$ are the residual meridional and vertical velocities; $\overline{u}$ and $\overline{b}$ are the Eulerian-mean zonal velocity and buoyancy; and $\overline{v'b'}$ is the meridional eddy buoyancy flux, where eddies are defined as a deviation from the Eulerian zonal mean. Also, τ is the zonal kinematic stress, Δp is the pressure difference (divided by density) across the basin (this is zero in the channel), L_x is the zonal extent of the basin, f is the Coriolis frequency, and κ_v is the diapycnal mixing. Horizontal friction and diffusion terms, eddy momentum fluxes, and nonlinear terms are neglected.

The residual velocity $(v^\dagger, w^\dagger)$ can be expressed in terms of a streamfunction as

$$(v^\dagger, w^\dagger) = (-\partial_z \psi^\dagger, \partial_y \psi^\dagger), \tag{2.5}$$

where $\psi^\dagger$ is the residual streamfunction. In the TEM framework, the residual streamfunction is sum of the Eulerian-mean streamfunction $\overline{\psi}$ and the eddy-induced streamfunction ψ^*, $\psi^\dagger = \overline{\psi} + \psi^*$. In this framework, it is the residual streamfunction, not the Eulerian streamfunction, that is solved for. The buoyancy fluxes then appear in (2.1) (i.e., in the momentum equation), and we parameterize them as

$$\overline{v'b'} = K_e \partial_y \overline{b}, \tag{2.6}$$

where K_e is an eddy diffusivity. Such an eddy parameterization is chosen because it is rational, simple, and commonly used. The theory presented here can in principle be extended to other forms of eddy parameterization. Note that eddy buoyancy fluxes act adiabatically, and the parameterization is similar to that of Gent and McWilliams (1990). If needed, the eddy-induced streamfunction can then be diagnosed using

$$\psi^* = -\frac{\overline{v'b'}}{\partial_z \overline{b}} = K_e s_b, \tag{2.7}$$

where $s_b = -\partial_y \overline{b}/\partial_z \overline{b}$ is the slope of the mean buoyancy surfaces.

There are potentially two quite different dynamical regions of the domain (Fig. 3): the circumpolar channel and the enclosed basin north of the channel. In the channel, where flow is not blocked by topography, the pressure difference across the basin Δp is zero. Using (2.5) and (2.7) and integrating Eq. (2.1) from an arbitrary depth below the mixed layer z, where stress τ is assumed to vanish, to the surface, where τ is equal to the wind stress τ_w, we obtain (and as noted previously by Johnson and Bryden 1989)

$$\psi^\dagger = -\frac{\tau_w}{f} + K_e s_b. \tag{2.8}$$

Hence, the residual circulation throughout the channel is a superposition of the wind-driven and the eddy-induced circulations. Using (2.5) and dividing Eq. (2.4) by $\partial_z \overline{b}$, the advection–diffusion equation for buoyancy can be rewritten as

$$\partial_y \psi^\dagger + s_b \partial_z \psi^\dagger = \kappa_v \frac{\partial_{zz} \overline{b}}{\partial_z \overline{b}}, \tag{2.9}$$

where terms on the left-hand side represent the adiabatic along-isopycnal flow and the term on the right is the diabatic cross-isopycnal flow.

Equations (2.8) and (2.9) describe the buoyancy distribution $\overline{b}$ and the residual overturning circulation $\psi^\dagger$ within the channel. For the typical circulation in the Southern Ocean driven by the westerly winds, surface buoyancy distribution across the channel, set in the mixed layer, is mapped through interior of the channel to its northern edge. To complete the problem, boundary conditions at the base of the mixed layer and at the northern edge of the channel need to be specified. At the base of the mixed layer, at $z = 0$, we assume that buoyancy distribution is prescribed,

$$\overline{b}\big|_{z=0} = b_0(y). \tag{2.10}$$

At the northern edge of the channel, at $y = 0$, both the buoyancy and the overturning circulation in the channel are required to match to those in the region north of the channel, as we now describe.

In the region north of the channel, we consider buoyancy surfaces that outcrop to the surface of the ocean only within the latitudes of the circumpolar channel. That is, in this paper, we will consider only the case with no source of deep water in the Northern Hemisphere. The model is thus relevant to the Pacific Ocean or the lower cell of the Atlantic Ocean overturning circulation. The buoyancy distribution and the overturning circulation in the region north of the channel have to satisfy buoyancy advection–diffusion Eq. (2.4). Assuming that the buoyancy surfaces north of the channel are horizontal [i.e., $\overline{b} = \overline{b}(z)$], (2.4) becomes a vertical advective–diffusive balance,

$$\partial_y \psi^\dagger \partial_z \overline{b} = \kappa_v \partial_{zz} \overline{b}, \tag{2.11}$$

where $\psi^\dagger = \overline{\psi}$ because $\psi^* = 0$ for flat isopycnals with $s_b = 0$.

Imposing a boundary condition of no flow across the northern boundary of the domain, Eq. (2.11) can be integrated from the northern boundary of the domain, at $y = L$, to the northern edge of the channel, at $y = 0$,

$$\psi^{\dagger}\big|_{y=0} = -\kappa_v L \frac{\partial_{zz}\overline{b}}{\partial_z \overline{b}}. \tag{2.12}$$

This equation describes the rate of the overturning circulation driven by the diapycnal mixing across the deep stratification in the basin away from the channel. Equation (2.12) is the northern boundary condition for the dynamics in the channel, and by satisfying it the buoyancy distribution and the overturning circulation at the northern edge of the channel become consistent with the advective–diffusive dynamics in the region north of the channel. We note that if $\kappa_v = 0$ everywhere then the residual circulation is also zero. However, if the dynamics within the channel are adiabatic (i.e., if κ_v is sufficiently small and the effects of diffusion are negligible), the residual circulation in the channel need not be zero if diffusion is nonnegligible in the basin.

The overturning circulation must cross isopycnals in the mixed layer of the channel to close the circulation (3). Cross-isopycnal flow in the mixed layer is balanced by the surface buoyancy flux $B(y)$. The surface buoyancy flux required to balance the circulation can be found from (2.4), integrating it from the base of the mixed layer at $z = 0$, where buoyancy flux $\kappa_v \partial_z \overline{b} \approx 0$, to the surface of the ocean, where $\kappa_v \partial_z \overline{b} = B(y)$,

$$B = \psi^{\dagger}\big|_{z=0} \partial_y b_0. \tag{2.13}$$

Hence, the surface buoyancy flux in our theoretical model is a part of the solution where it is required to balance the overturning circulation in the mixed layer driven by the diapycnal mixing in the interior of the ocean.

In summary, Eqs. (2.8) and (2.9) combined with the surface boundary condition in (2.10) and the northern edge boundary condition in (2.12) represent a complete set of equations describing the stratification and overturning circulation. Collecting them together for convenience the equations are

$$\partial_y \psi^{\dagger} + s_b \partial_z \psi^{\dagger} = \kappa_v \frac{\partial_{zz}\overline{b}}{\partial_z \overline{b}}, \tag{2.14}$$

$$\psi^{\dagger} = -\frac{\tau_w}{f} + K_e s_b, \tag{2.15}$$

$$\psi^{\dagger}\big|_{y=0} = -\kappa_v L \frac{\partial_{zz}\overline{b}}{\partial_z \overline{b}}, \quad \text{and} \tag{2.16}$$

$$\overline{b}\big|_{z=0} = b_0(y). \tag{2.17}$$

The equations describe the buoyancy distribution $\overline{b}$ and the residual overturning circulation $\psi^{\dagger}$ on isopycnals that outcrop only in the circumpolar channel. The overturning circulation in the basin away from the channel is balanced by the downward diffusion across horizontal buoyancy surfaces and is matched to the residual circulation in the channel, which is set by a balance between the wind-driven and eddy-induced overturning circulations. We note that the dynamics in the two regions are necessarily coupled. For instance, higher diapycnal mixing in the basin away from the channel drives stronger overturning circulation across a given stratification and therefore requires stronger residual circulation in the channel to match. Stronger residual circulation in the channel, in turn, requires stronger eddy-induced circulation (wind-driven circulation is fixed by the wind), which causes isopycnals in the channel and thus stratification in the basin away from the channel to change.

c. Nondimensionalization and scaling

We nondimensionalize both the governing equations and boundary conditions using the following characteristic scales:

$$z = h\hat{z}, \quad y = l\hat{y}, \quad \tau_w = \tau_0 \hat{\tau}_w,$$
$$f = f_0 \hat{f}, \quad \psi^{\dagger} = \frac{\tau_0}{f_0}\hat{\psi}, \quad s_\rho = \frac{h}{l}\hat{s}_\rho,$$

where h is the characteristic vertical scale of stratification (to be determined), l is the width of the channel, and τ_0 is the magnitude of the wind stress. Note, that the rate of the overturning circulation is scaled with the characteristic rate of the wind-driven circulation.

In a nondimensional form, Eqs. (2.14)–(2.16) can be written as

$$\partial_y \hat{\psi} + \hat{s}_b \partial_z \hat{\psi} = \varepsilon \left(\frac{l}{L}\right) \frac{\partial_{zz}\hat{b}}{\partial_z \hat{b}}, \tag{2.18}$$

$$\hat{\psi} = -\frac{\hat{\tau}_w}{\hat{f}} + \Lambda \hat{s}_b, \quad \text{and} \tag{2.19}$$

$$\hat{\psi}\big|_{y=0} = -\varepsilon \frac{\partial_{zz}\hat{b}}{\partial_z \hat{b}}. \tag{2.20}$$

The variables with hats on are presumptively order one and

$$\Lambda = \frac{K_e}{\tau_0/f_0}\frac{h}{l} \quad \text{and} \quad \varepsilon = \frac{\kappa_v}{\tau_0/f_0}\frac{L}{h} \tag{2.21a,b}$$

are the nondimensional parameters, the ''eddyness'' and ''diffusiveness,'' respectively, that give the ratios of the

eddy-induced and diffusion-driven circulation to the wind-driven overturning circulation, respectively. The ratio l/L is a geometric factor that affects the relative importance of diapycnal mixing in the channel and in the region north of the channel for the overturning circulation.

Choosing values of $\kappa_v = 10^{-5}$ m^2 s^{-1}, $K_e = 10^3$ m^2 s^{-1}, $\tau_0 = 0.1$ N m^{-2}, $f_0 = 10^{-4}$ s^{-1}, $\rho_0 = 10^3$ kg m^{-3}, $L =$ 10 000 km, $l =$ 1000 km, and $h = 1$ km typical for the middepth ocean, we get

$$\Lambda = 1, \quad \varepsilon = 0.1, \quad \text{and} \quad \frac{l}{L} = 0.1.$$

Hence, the overturning circulation and stratification at middepth in the ocean are primarily controlled by the wind and eddies in the channel, $\Lambda = O(1)$, with diapycnal mixing playing a minor role, $\varepsilon \ll 1$. Diapycnal mixing in the channel is much less important than the diapycnal mixing in the basin north of the channel, $l/L \ll 1$.

The nondimensional numbers Λ and ε are not independent of each other for they both depend on the vertical scale of stratification h, which is a part of the solution. In the limit of $\varepsilon \ll 1$, Λ must be of $O(1)$ for the eddy-induced circulation to balance the wind-driven circulation in (2.19) corresponding to the characteristic vertical scale of stratification,

$$h = \frac{\tau_0/f_0}{K_e} l. \tag{2.22}$$

The scaling for h implies that stronger surface winds result in the deeper penetration of stratification into the ocean. Using (2.22) as the vertical scale h, the nondimensional number ε given in (2.21b) can be written completely in terms of the external parameters of the problem as

$$\varepsilon = \frac{\kappa_v K_e}{(\tau_0/f_0)^2} \frac{L}{l}. \tag{2.23}$$

The corresponding scaling for the rate of the overturning circulation Ψ in the limit of $\varepsilon \ll 1$ can be found from (2.20) as

$$\Psi = \varepsilon \frac{\tau_0}{f_0} = \kappa_v \frac{K_e}{\tau_0/f_0} \frac{L}{l}. \tag{2.24}$$

Dimensionally, we may obtain (2.24) by noting that in the weak diffusion limit the balance in the momentum Eq. (2.15) is

$$\frac{\tau_w}{f} \approx K_e s_b, \tag{2.25}$$

so that

$$h \approx \frac{\tau_w l}{K_e f}. \tag{2.26}$$

The advective–diffusive balance (2.16) implies that

$$\Psi = \frac{\kappa_v L}{h}, \tag{2.27}$$

and using (2.26) in (2.27) gives (2.24).

The rate of the overturning circulation is linearly proportional to the diapycnal mixing κ_v, as it is expected from the advective–diffusive buoyancy balance (2.20) when the buoyancy distribution itself is independent of diapycnal mixing. The circulation also depends on the wind and eddies in the channel, because these set stratification throughout the ocean and thus modify the rate of the overturning circulation. It is inversely proportional to the wind: stronger wind over the channel stretches stratification from the upper to the deep ocean, decreases its curvature, and thus reduces diffusion-driven overturning circulation. A more detailed analytic solution in the limit of $\varepsilon \ll 1$ is described in the next section.

If the diapycnal diffusivity is sufficiently large, then $\varepsilon \gg 1$, and this limit may be of relevance for the abyssal ocean. The effect of diapycnal mixing in the basin north of the channel on the overturning circulation and stratification then becomes bigger than the wind effect. In this limit, the nondimensional number Λ must be $O(\varepsilon)$ for the eddy-induced circulation in the channel to match to the diffusion-driven circulation in the basin north of the channel. The leading-order balance in Eqs. (2.19) and (2.20) becomes,

$$\hat{\psi} = \Lambda \hat{s}_b \quad \text{and} \tag{2.28}$$

$$\hat{\psi}\big|_{y=0} = -\varepsilon \frac{\partial_{zz} \hat{b}}{\partial_z \hat{b}}. \tag{2.29}$$

From $\Lambda = O(\varepsilon)$, we obtain that the vertical scale of stratification is

$$h = \sqrt{\frac{\kappa_v}{K_e} L l}. \tag{2.30}$$

Using (2.30) in (2.21b), we obtain

$$\varepsilon = \left[\frac{\kappa_v K_e}{(\tau_0/f_0)^2} \frac{L}{l} \right]^{1/2}, \tag{2.31}$$

which is the square root of the expression (2.23) that holds in the weak mixing case.

Thus, in the $\varepsilon \gg 1$ limit, the stratification depth scale h scales with diapycnal mixing as $\kappa_v^{1/2}$, and this is because diapycnal mixing not only mixes across deep stratification but also modifies the stratification itself. The corresponding scaling for the rate of the overturning circulation Ψ is then found to be, from (2.27) and (2.30),

$$\Psi = \sqrt{\kappa_v K_e \frac{L}{l}}. \tag{2.32}$$

The rate of the overturning circulation is independent of the wind stress τ_0 in this limit. It is controlled by diapycnal mixing deepening isopycnals in the basin away from the channel and thus steepening isopycnals in the channel and by mesoscale eddies slumping isopycnals in the circumpolar channel. Scaling of the rate of the overturning circulation with diapycnal mixing as $\kappa_v^{1/2}$ is consistent with the estimates previously given by Kamenkovich and Goodman (2000) and Ito and Marshall (2008).

3. Analytical solution in the weak diffusion limit

Equations (2.18)–(2.20) are nonlinear and cannot be solved analytically for an arbitrary choice of parameters, wind, and surface buoyancy distribution. However, analytical progress can be made in the limit of weak diapycnal mixing.

a. Asymptotics

In the limit of $\varepsilon \ll 1$, the solution to Eqs. (2.18)–(2.20) can be found by a regular expansion method,

$$\hat{\psi} = \hat{\psi}^{(0)} + \varepsilon\hat{\psi}^{(1)} + O(\varepsilon^2) \quad \text{and}$$

$$\hat{b} = \hat{b}^{(0)} + \varepsilon\hat{b}^{(1)} + O(\varepsilon^2).$$

Substituting these expansions in Eqs. (2.18)–(2.20) and assuming that $l/L = O(\varepsilon)$, at $O(\varepsilon^0)$ we obtain

$$\partial_y\hat{\psi}^{(0)} + \hat{s}_b^{(0)}\partial_z\hat{\psi}^{(0)} = 0, \tag{3.1}$$

$$\hat{\psi}^{(0)} = -\frac{\hat{\tau}_w}{\hat{f}} + \Lambda\hat{s}_b^{(0)}, \quad \text{and} \tag{3.2}$$

$$\hat{\psi}^{(0)}\big|_{y=0} = 0, \tag{3.3}$$

where $\hat{s}_b^{(0)} = -\partial_y\hat{b}^{(0)}/\partial_z\hat{b}^{(0)}$ is the leading-order isopycnal slope. From Eq. (3.1) and the boundary condition (3.3), we find that, to leading order, the residual overturning circulation throughout the entire ocean is zero:

$$\hat{\psi}^{(0)} = 0. \tag{3.4}$$

The residual overturning circulation in the channel is closed in the basin away from the channel,where it is balanced by the downward diffusion (Fig. 3). In the limit when diffusion is weak, $\varepsilon \ll 1$, the residual circulation becomes weak, $O(\varepsilon)$, compared to the wind-driven circulation. From (3.2), it follows that at $O(\varepsilon^0)$ there is a cancellation between the wind-driven and eddy-induced circulation resulting in the leading-order isopycnal slope

$$\hat{s}_b^{(0)} \equiv -\frac{\partial_y\hat{b}^{(0)}}{\partial_z\hat{b}^{(0)}} = \Lambda^{-1}\frac{\hat{\tau}_w}{\hat{f}}. \tag{3.5}$$

Equation (3.5) is a first-order linear partial differential equation for buoyancy $\hat{b}^{(0)}$, which can be solved by a method of characteristics using the surface buoyancy boundary condition. The surface buoyancy distribution is mapped through interior of the channel to its northern boundary along characteristics that are given by

$$z = \Lambda^{-1}\int_0^y \frac{\hat{\tau}_w}{\hat{f}}\,dy' + C, \tag{3.6}$$

where C is a constant. Hence, in the limit of weak diapycnal mixing, the residual overturning circulation at lowest order [i.e., $O(\varepsilon^0)$] is zero and the buoyancy distribution across the channel and therefore throughout the basin is set by the wind and eddies in the channel.

At next order, collecting $O(\varepsilon^1)$ terms, we obtain

$$\partial_y\hat{\psi}^{(1)} + \hat{s}_b^{(0)}\partial_z\hat{\psi}^{(1)} = 0, \tag{3.7}$$

$$\hat{\psi}^{(1)} = \Lambda\hat{s}_b^{(1)}, \quad \text{and} \tag{3.8}$$

$$\hat{\psi}^{(1)}\big|_{y=0} = -\frac{\partial_{zz}\hat{b}^{(0)}}{\partial_z\hat{b}^{(0)}}. \tag{3.9}$$

The boundary condition (3.9) gives rise to an $O(\varepsilon^1)$ overturning circulation driven by diapycnal mixing in the basin away from the channel acting on the $O(\varepsilon^0)$ buoyancy distribution, determined by the wind and eddies in the channel. According to Eq. (3.7), this overturning circulation adiabatically follows $O(\varepsilon^0)$ isopycnals from the northern edge of the channel to the base of the mixed layer. An $O(\varepsilon^1)$ correction to the leading-order isopycnal slope in the channel can be found from Eq. (3.8).

b. Analytic solution in a special case

Analytical solutions to the $O(\varepsilon^0)$ and $O(\varepsilon^1)$ equations can be found if relatively simple wind and surface buoyancy distributions, allowing to evaluate the integral in (3.6), are specified. Here, we use dimensional form of

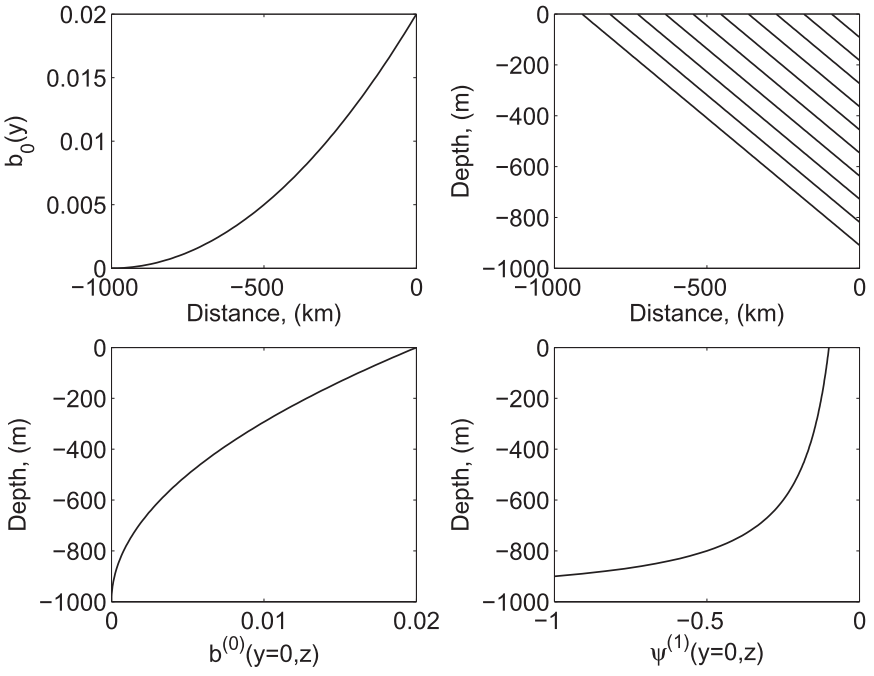

FIG. 4. Idealized analytical solutions: (top left) prescribed surface buoyancy $b_0(y)$; (top right) characteristics; (bottom left) buoyancy at the northern edge of the channel $b^{(0)}(z)$; and (bottom left) overturning streamfunction at the northern edge of the channel $\psi^{(1)}(z)$.

the governing equations and assume that both the wind and the Coriolis frequency are constant across the channel, τ_0 and f_0, respectively, and the surface buoyancy is prescribed as

$$b_0(y) = \Delta b\left(1 + \frac{y}{l}\right)^2, \tag{3.10}$$

where Δb is buoyancy change across the channel. This choice is somewhat arbitrary and made here to illustrate the dependence of the model solution on the parameters of the problem.

From (3.5), the slope of isopycnals in the channel is constant and equal to

$$s_b^{(0)} = \frac{\tau_0/f_0}{K_e}. \tag{3.11}$$

The surface buoyancy distribution is mapped through interior of the channel to its northern boundary along characteristics, which are found from (3.6) as

$$z = \frac{\tau_0/f_0}{K_e}(y - y_0), \tag{3.12}$$

where y_0 is a constant. If wind and Coriolis parameter are constant, then characteristics are straight lines (Fig. 4). Mapping surface buoyancy in (3.10) through the channel along characteristics in (3.12), the $O(\varepsilon^0)$ buoyancy distribution within the channel becomes

$$b^{(0)}(y,z) = \Delta b\left(1 + \frac{y}{l} - \frac{K_e}{\tau_0/f_0}\frac{z}{l}\right)^2. \tag{3.13}$$

At the northern edge of the channel, at $y = 0$, buoyancy increases quadratically from the deep ocean toward the surface (Fig. 4) with a characteristic vertical scale given by (2.22).

Now, the rate of the $O(\varepsilon^1)$ overturning circulation at the northern edge of the channel can be found from Eq. (3.9) as

$$\psi^{(1)}\big|_{y=0} = \kappa_v \frac{K_e}{\tau_0/f_0}\frac{L}{l}\left(1 - \frac{K_e}{\tau_0/f_0}\frac{z}{l}\right)^{-1}. \tag{3.14}$$

Finally, the overturning circulation throughout the channel can be found using Eq. (3.7) as

$$\psi^{(1)}(y,z) = \kappa_v \frac{K_e}{\tau_0/f_0}\frac{L}{l}\left(1 + \frac{y}{l} - \frac{K_e}{\tau_0/f_0}\frac{z}{l}\right)^{-1}. \tag{3.15}$$

The overturning circulation has a magnitude given by (2.24) and varies with depth on the same vertical scale h as the buoyancy distribution (Fig. 4). The solutions in (3.13) and (3.15) describe the distribution of buoyancy

and overturning streamfunction within the channel, which are consistent with the adiabatic dynamics in the channel and the diabatic dynamics in the region north of the channel.

In the channel, overturning circulation is closed in the mixed layer. The corresponding surface buoyancy flux required to balance the cross-isopycnal flow in the mixed layer can be found from (2.13),

$$B = 2\kappa_v \frac{\Delta b}{l} \frac{K_e}{\tau_0/f_0} \frac{L}{l}. \tag{3.16}$$

It is proportional to diapycnal diffusivity and the buoyancy gradient across the channel and inversely proportional to the wind. Stronger wind over the channel reduces the rate of the overturning circulation, which, in turn, requires smaller surface buoyancy flux to cross isopycnals in the mixed layer.

Analytical solutions can in fact also be found for more realistic profiles of wind and surface buoyancy distribution across the channel. These solutions are characterized by the same parameter dependence as the one described here but become algebraically complex and less informative and thus are not shown here.

4. Numerical solution of theoretical equations

In this section, we numerically solve the governing equations of our theory (2.14)–(2.17). This allows us to explore solutions in a broad parameter range and enables a more direct comparison to be made with simulations using an ocean general circulation model, as described later.

a. Numerical solver setup

The equations are solved by integrating forward a time-dependent form of the buoyancy advection–diffusion Eq. (2.14),

$$\partial_t \overline{b} - \partial_z \psi^\dagger \partial_y \overline{b} + \partial_y \psi^\dagger \partial_z \overline{b} = \kappa_v \partial_{zz} \overline{b}, \tag{4.1}$$

using the appropriate boundary conditions and the advective streamfunction given by (2.15). The equations are discretized using finite differencing on a staggered Cartesian grid in the domain of the circumpolar channel, which extends from the southern boundary at $y = -1000$ km to the northern edge of the channel at $y = 0$ and from the bottom at $z = -4$ km to the base of the mixed layer at $z = 0$ with the meridional and vertical grid spacings of 25 km and 25 m, respectively. In addition to the northern edge and the surface boundary conditions in (2.16) and (2.17), we also impose a no-flux and zero streamfunction boundary conditions at the bottom and the southern boundary of the domain. Eddies are parameterized using a Gent–McWilliams type of parameterization with the eddy diffusivity of $K_e = 1000\ \mathrm{m^2\ s^{-1}}$ in the form of the boundary-value problem (Ferrari et al. 2010), which allows for a smooth transition of the eddy streamfunction to the weakly stratified regions, and in all the cases we report the evolution converges to an absolute steady state.

Although numerical solutions can be found for almost arbitrary surface boundary conditions and problem parameters, here we discuss solutions obtained for the same surface buoyancy distributions (3.10) with $\Delta b = 2 \times 10^{-2}\ \mathrm{m\ s^{-2}}$ and constant wind stress $\tau_w = 0.1\ \mathrm{N\ m^{-2}}$ as used in the previous section. Numerical solution in the channel can be extended analytically to the basin north of the channel by integrating the vertical advective–diffusive balance (2.11) from the northern edge of the channel at $y = 0$ to a latitude y,

$$\psi^\dagger = -\kappa_v L \frac{\partial_{zz}\overline{b}}{\partial_z \overline{b}} \left(1 - \frac{y}{L}\right) \quad 0 < y < L, \tag{4.2}$$

where $\overline{b}$ is the buoyancy at the northern edge of the channel projected horizontally across the basin.

b. Buoyancy and overturning circulation

The meridional buoyancy distribution $\overline{b}$ and the residual overturning circulation $\psi^\dagger$ both in the channel and in the basin north of the channel computed for three different values of diapycnal mixing are shown in Fig. 5. Values of diapycnal mixing are chosen to correspond to a weak diapycnal mixing limit of $\varepsilon = 0.01$, to a moderate diapycnal mixing limit of $\varepsilon = 0.1$, and to a strong diapycnal mixing limit of $\varepsilon = 1$.

With $\varepsilon = 0.01$, the overturning circulation is weak, with $|\psi| \sim 0.1\ \mathrm{m^2\ s^{-1}}$, throughout the ocean. According to the theory, the diffusion-driven circulation should be small, $O(\varepsilon)$, compared to the wind-driven circulation in this limit. The isopycnal slopes in the channel are set by a balance between the wind-driven and eddy-induced circulation, with the two canceling to give a very small residual circulation. The surface buoyancy distribution across the channel is mapped on its northern edge resulting in stratification penetrating down to about 1-km depth, consistent with the analytical solution given in (3.13) and shown in Fig. 4. Analytical solutions for the buoyancy and the overturning streamfunction at the northern edge of the channel are compared with the $\varepsilon = 0.01$ numerical solutions in Fig. 6. As expected in the limit of $\varepsilon \ll 1$, analytical and numerical solutions match very well in the upper 1 km. The overturning streamfunction solutions begin to diverge deeper that 1 km

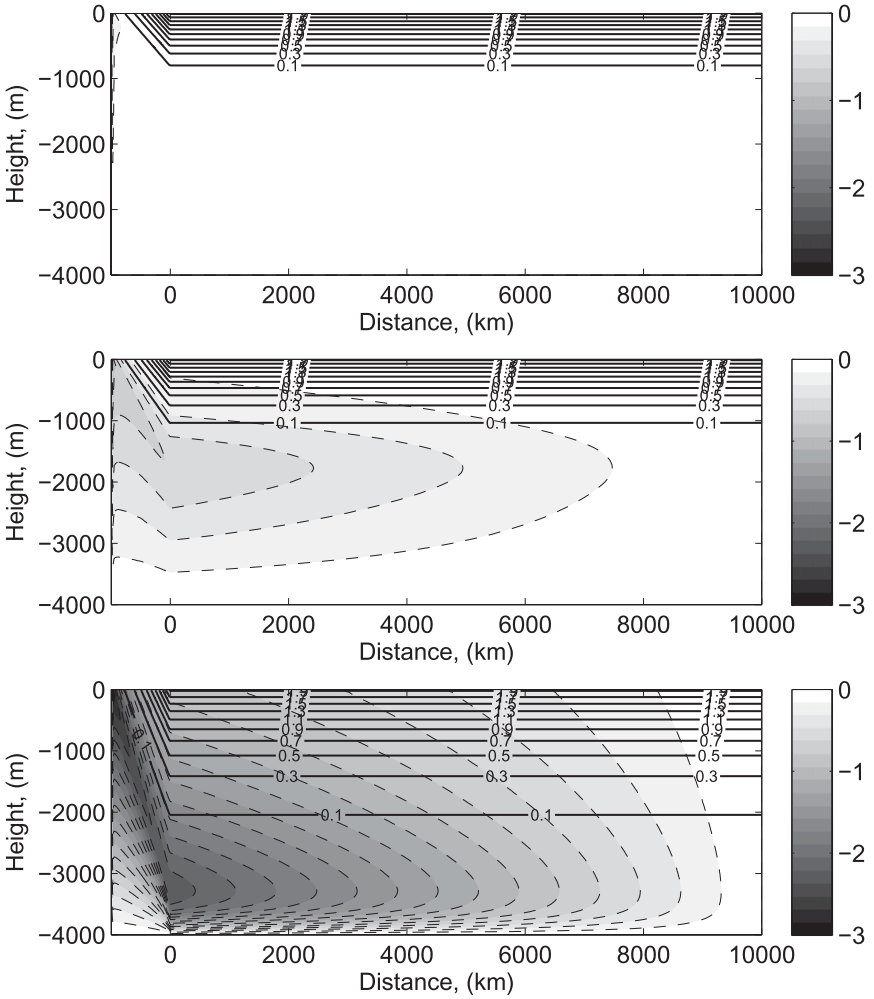

FIG. 5. Buoyancy distribution $\overline{b}$ (10^{-2} m s^{-2}) (solid lines) and the residual overturning circulation $\psi^{\dagger}$ (m^2 s^{-1}) (dashed lines) computed numerically in the circumpolar channel and extended analytically to the basin north of the channel for different values of diapycnal mixing: (top) 10^{-6} m^2 s^{-1}, (middle) 10^{-5} m^2 s^{-1}, and (bottom) 10^{-4} m^2 s^{-1}, corresponding to $\varepsilon = 0.01$, $\varepsilon = 0.1$, and $\varepsilon = 1$, respectively.

because the numerical solution exists throughout the entire water column and thus matches the stratified region in the upper 1 km to the unstratified region below, whereas the analytical solution is found by mapping surface buoyancy along isopycnals and exists only in the stratified region.

In case of a moderate diapycnal diffusivity, with $\kappa_v = 10^{-5}$ m^2 s^{-1}, corresponding to $\varepsilon = 0.1$, the overturning circulation increases by an order of magnitude but still remains small compared to the wind-driven circulation. Consistent with the theory, the slope of isopycnals in the channel as well as their depth in the basin away from the channel remain largely unchanged (Fig. 5). In this limit, wind and eddies set the slope of isopycnals in the channel and therefore stratification throughout the ocean, whereas diapycnal mixing acts on this stratification primarily in the basin away from the channel and drives the overturning circulation.

Finally, in the case of strong diapycnal mixing, corresponding to $\varepsilon = 1$, both the residual overturning circulation and stratification throughout the domain are affected by diapycnal mixing in the basin: isopycnals extend significantly deeper into the ocean. In this limit, isopycnal slopes in the channel and stratification throughout the ocean are controlled not only by the wind and eddies in the channel but also by diapycnal mixing in the basin away from the channel.

The overturning circulation in both regimes can be described as consisting of four dynamically different regions illustrated schematically in Fig. 3: (i) downwelling

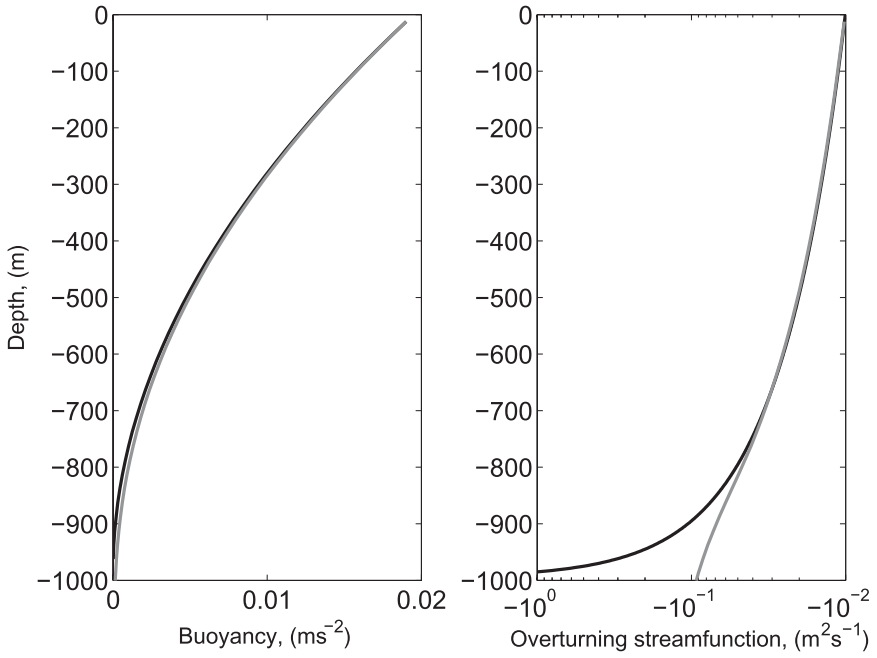

FIG. 6. Vertical profiles of buoyancy (m s^{-2}) and overturning circulation (m^2 s^{-1}) in the upper 1 km at the northern edge of the channel at $y = 0$ from analytical (black) and numerical (gray) solution for $\kappa_v = 10^{-6}$ m^2 s^{-1}.

in the narrow convective region at the southern boundary of the domain, (ii) cross-isopycnal upwelling in the basin away from the channel, (iii) along-isopycnal upwelling in the circumpolar channel, and (iv) the cross-isopycnal flow in the mixed layer. Although there is a small cross-isopycnal circulation within the channel, it is significantly smaller than the cross-isopycnal circulation in the basin. The numerical solution computed with a boundary condition of a zero residual streamfunction at the northern edge of the channel (not shown here)—that is, with no basin north of the channel—results in an order of magnitude smaller residual overturning circulation in the channel.

c. Parameter sensitivity

We now quantitatively describe the dependence of the numerical solution on the parameters of the problem, particularly the transition of the solution from the weak to strong mixing regimes. We test the analytic scalings for the vertical scale of stratification h and the rate of the overturning circulation Ψ described in section 2 against numerical solutions computed for different values of diapycnal diffusivity κ_v and wind stress τ_w.

Figures 7 and 8 show the dimensional isopycnal depth h and the rate of the overturning circulation Ψ as a function of the diapycnal diffusivity, for three different values of the wind stress. The isopycnal depth is defined here as the depth of the 10^{-2} m^2 s^{-1} buoyancy isoline at the northern edge of the channel. The rate of the overturning circulation is defined as the mean overturning streamfunction at the northern edge of the channel above 10^{-2} m^2 s^{-1} buoyancy isoline. Although the choice of the buoyancy isoline is a little arbitrary, the results are insensitive to this choice.

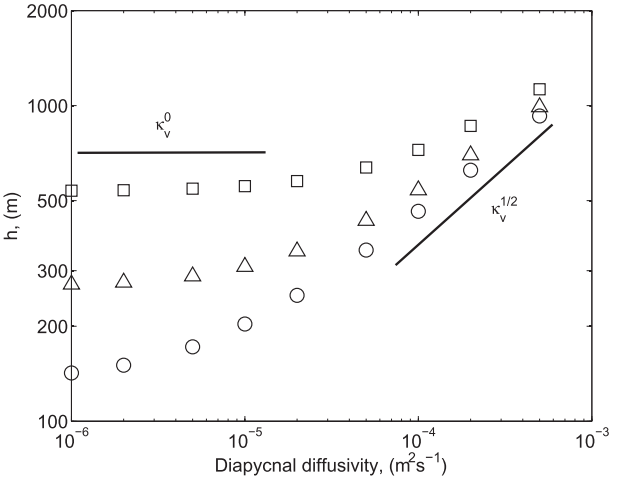

FIG. 7. Depth of 10^{-2} m s^{-2} buoyancy isoline (m) plotted as a function of diapycnal diffusivity κ_v. Markers correspond to numerical solutions obtained for three values of wind stress: τ_w = 0.05 N m^{-2} (circles), τ_w = 0.1 N m^{-2} (triangles), and τ_w = 0.2 N m^{-2} (squares).

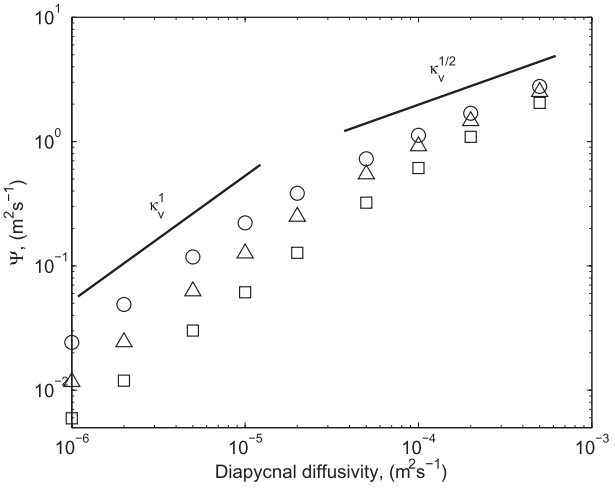

FIG. 8. Rate of the overturning circulation ($m^2\ s^{-1}$) plotted as a function of diapycnal diffusivity κ_v. Markers correspond to numerical solutions obtained for three values of wind stress: τ_w = 0.05 N m^{-2} (circles), τ_w = 0.1 N m^{-2} (triangles), and τ_w = 0.2 N m^{-2} (squares).

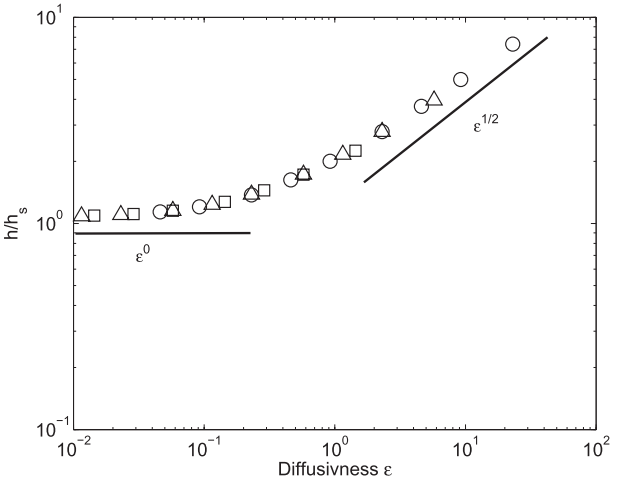

FIG. 9. Depth of 10^{-2} m s^{-2} buoyancy isoline normalized by theoretical prediction h_S from (2.22) and plotted as a function of the nondimensional parameter ε. Markers correspond to different numerical solutions obtained by varying diapycnal diffusivity κ_v from 10^{-6} to 5×10^{-4} $m^2\ s^{-1}$ for 3 values of wind stress: τ_w = 0.05 N m^{-2} (circles), τ_w = 0.1 N m^{-2} (triangles), and τ_w = 0.2 N m^{-2} (squares).

As can be seen in the figures, the depth increases with the wind and the diffusivity, whereas the circulation increases with the diffusivity but decreases with the wind. In the limit of $\varepsilon \ll 1$, which corresponds to small values of diapycnal mixing or large values of wind stress, the scaling (2.22) predicts the isopycnal depth to be independent of the diapycnal mixing and to be set by the wind and eddies in the circumpolar channel, and results are consistent with this (Fig. 7, left). The overturning circulation is driven by diapycnal mixing acting across essentially fixed stratification and hence scales linearly with κ_v [see (2.24)]; the results shown in Fig. 8 at the smaller values of κ_v are consistent with this.

In contrast, in the limit of $\varepsilon \gg 1$, mixing has a strong effect on stratification. The dimensional scalings (2.30) and (2.32) predict that both the isopycnal depth and the rate of the overturning circulation should scale as $\kappa_v^{1/2}$, and the results shown in Figs. 7 and 8 at the larger values of κ_v are consistent with this.

To test still more quantitatively whether the scalings apply, we normalize the depth h and the circulation Ψ by the corresponding theoretical scalings (2.22) and (2.24) and plot the results as a function of the nondimensional parameter ε diagnosed from numerical solutions for different values of diapycnal mixing κ_v and wind stress τ_w. The results, shown in Figs. 9 and 10 , show a pleasing collapse of the results onto single lines. For small diffusiveness, just a little algebra reveals that the nondimensional depth and nondimensional circulation should be independent of ε and the numerical results reflect this. At high diffusiveness, the depth should scale as $\varepsilon^{1/2}$ and the circulation as $\varepsilon^{-1/2}$ and these are satisfied by the numerical results. The transition between the two regimes takes place at $\varepsilon \approx 0.5$–1.0.

5. Tests with a numerical ocean model

a. Numerical experiments

Finally, to further test the scalings derived in section 2, we have performed some calculations with a numerical ocean general circulation model. We use the Modular Ocean Model (MOM) version 4.0c (Griffies et al. 2004). The model is configured in a single-basin flat-bottomed domain (as in Fig. 2) with a horizontal resolution of 2° × 2° and 20 vertical levels of thickness varying from 20 m at the top to 380 m at the bottom. The domain extends from 72°S to 0° across 60° of longitude. There is a full-depth zonally periodic channel between 72°S and 52°S. The effect of eddies is parameterized with a Gent–McWilliams-like scheme in the form of the boundary-value problem (Ferrari et al. 2010), and a uniform diapycnal diffusivity, with a value of $\kappa_v = 10^{-5}$ $m^2\ s^{-1}$ in the control case, is used.

The surface buoyancy flux is implemented via a restoring boundary condition on temperature, and salinity is set to a uniform constant. We use a thermal restoring coefficient of 47 W m^{-2} K^{-1} corresponding to a 10-day restoring time scale. We use a zonally uniform SST and wind stress (Fig. 11) constructed analytically based on the annual global zonal-mean observations from the

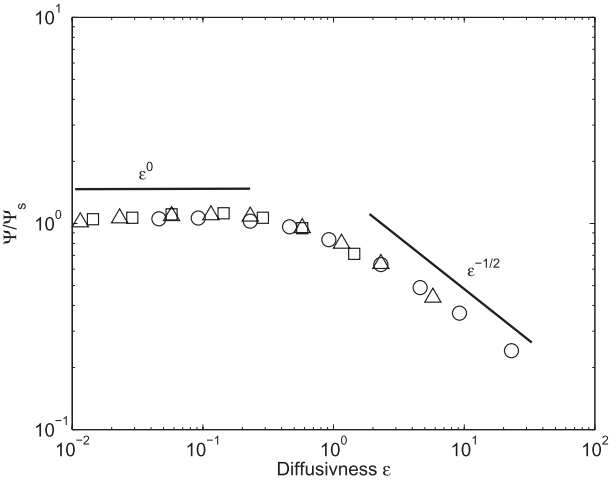

FIG. 10. Rate of the overturning circulation normalized by theoretical prediction Ψ_S from (2.24) and plotted as a function of the nondimensional parameter ε. Markers correspond to different numerical solutions obtained by varying diapycnal diffusivity κ_v from 10^{-6} to 5×10^{-4} m^2 s^{-1} for three values of wind stress: $\tau_w = 0.05$ N m^{-2} (circles), $\tau_w = 0.1$ N m^{-2} (triangles), and $\tau_w = 0.2$ N m^{-2} (squares).

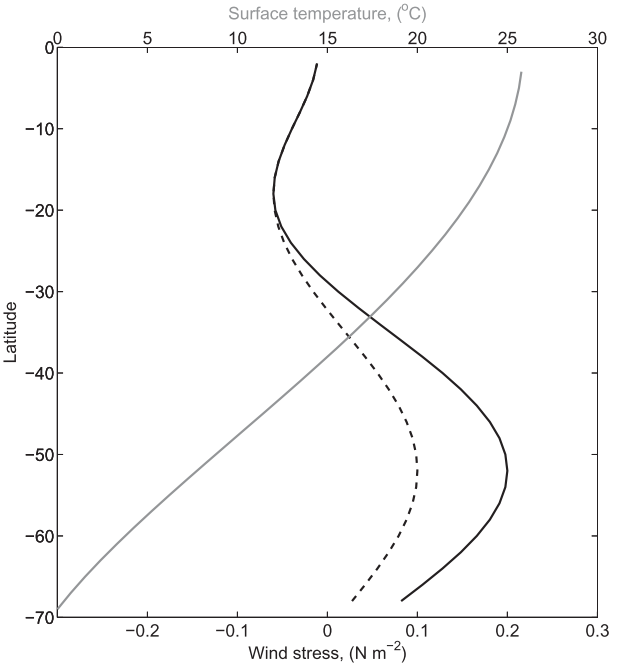

FIG. 11. The annual-mean zonally uniform wind stress (black) and SST restoring field (gray). Perturbed wind over the Southern Ocean is shown in dashed black line.

National Oceanographic Data Center (NODC) *World Ocean Atlas 2001* (Conkright et al. 2002) and the last 20 yr of the National Centers for Environmental Prediction–National Center for Atmospheric Research (NCEP–NCAR) reanalysis (Kalnay et al. 1996) for temperature and wind stress, respectively. The model is initialized from a state of rest and is spun up over 3000 yr until it reaches a steady state. Similar numerical model setups have been used to study the large-scale stratification and overturning circulation before (e.g., Vallis 2000; Henning and Vallis 2005; Ito and Marshall 2008; Wolfe and Cessi 2010).

We carried out two sets of experiments on sensitivity of the deep stratification and overturning circulation to diapycnal mixing and the wind stress. In the first set of experiments, we varied diapycnal diffusivity in the range from 10^{-6} to 10^{-3} m^2 s^{-1}, keeping all other parameters, including the wind stress, fixed. In the second set of experiments, the wind stress over the Southern Ocean was varied as shown in Fig. 11 with an amplitude spanning the range from 0.02 to 0.5 N m^{-2}, with diapycnal mixing and other parameters kept fixed.

In Fig. 12, we show zonally averaged sections of the residual circulation and temperature from two experiments corresponding to low and high diapycnal mixing values. In both experiments there is a deep overturning cell below roughly 1 km, away from the surface wind-driven overturning cells. Similar to the theoretical solution described in the previous section, the deep overturning cell consists of convection at the southern boundary of the domain, cross-isopycnal upwelling in the basin away from the channel, and largely isopycnal upwelling in the circumpolar channel. In the high mixing experiment, isopycnals extend significantly deeper into the ocean and the overturning rate is much stronger than in the experiment with low diapycnal mixing. We note that high diapycnal mixing affects not only the structure in the basin away from the channel but also the structure in the channel, where the slope of isopycnals in the circumpolar channel is greater in the high mixing experiment. Although the numerical ocean model is based on fully three-dimensional dynamics and includes many other features of the ocean circulation like the wind-driven gyres and frictional boundary layers, its overturning circulation in the circumpolar channel and in the deep ocean compares well both qualitatively (Fig. 5) and, as we show below, quantitatively with the theory.

b. Comparison with scalings

The sensitivity of the numerical ocean model to changes in diapycnal diffusivity and wind stress are shown in Fig. 13. The isopycnal depth is diagnosed as a depth of the 2°C zonally averaged isotherm in the region away from the channel, north of 30°S. The rate of the overturning circulation is diagnosed as an average of the residual circulation in the region north of 30°S and below the 5°C isotherm. The results show that both the

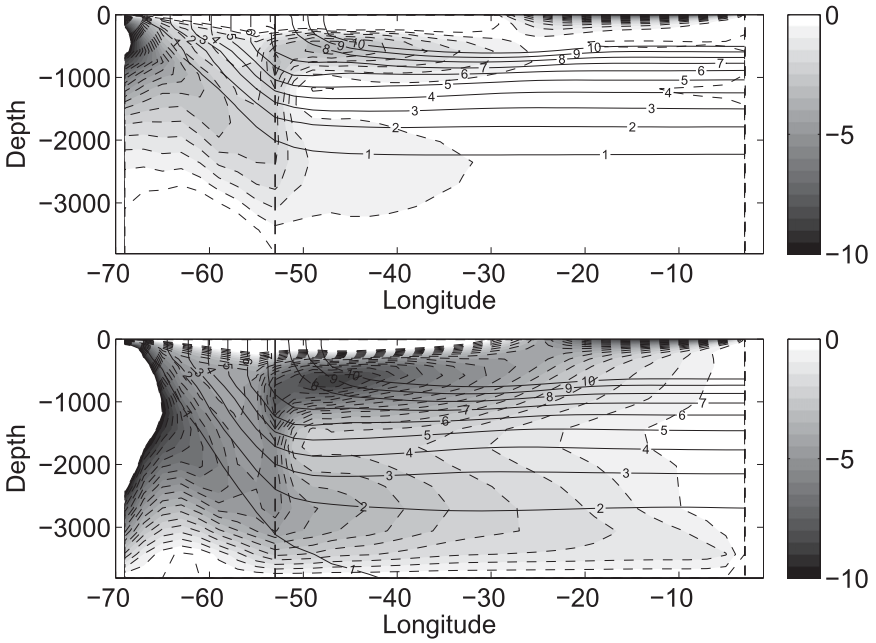

FIG. 12. Temperature isolines (°C) (solid lines) and the residual overturning circulation [in Sv (1 Sv $\equiv 10^6$ m^3 s^{-1})] (dashed lines) diagnosed from the ocean general circulation model experiments for two different values of diapycnal mixing: (top) 10^{-5} and (bottom) 10^{-4} m^2 s^{-1}.

isopycnal depth and the rate of the overturning circulation in the basin away from the channel are sensitive not only to diapycnal mixing but also to variation in the wind stress over the circumpolar channel. Consistent with the theory, in the limit of weak diapycnal mixing, $\varepsilon \ll 1$, the isopycnal depth becomes independent of diapycnal mixing κ_v, whereas the rate of the overturning circulation scales linearly with κ_v. In the limit of strong diapycnal mixing, $\varepsilon \gg 1$, both the isopycnal depth and the rate of the overturning circulation scale with κ_v as $\kappa_v^{1/2}$. The dependence of the numerical solution on the wind stress is also generally consistent with the theory. The isopycnal depth increases linearly with τ_w in the $\varepsilon \ll 1$ limit, whereas it is insensitive to the wind stress in $\varepsilon \gg 1$ limit. Similarly, the rate of the overturning circulation scales with wind stress as τ_w^{-1} in the $\varepsilon \ll 1$ limit and becomes independent of the wind stress in the $\varepsilon \gg 1$ limit, although we are not able to completely explore the extreme parameter regimes with the numerical ocean model.

6. Discussion and conclusions

a. Summary

In this paper, we have presented a theoretical model of deep stratification and meridional overturning circulation in a single-basin ocean with a circumpolar channel. The theory is based on a matching of the dynamics in the circumpolar channel with the dynamics in the basin north of the channel and includes the effects of wind, eddies, and diapycnal mixing. In parameter regimes that most closely correspond to the real ocean, the dynamics in the circumpolar channel are essentially adiabatic, whereas the dynamics in the basin are advective–diffusive and therefore diabatic. The theory explicitly predicts the deep stratification in terms of the surface forcing and other problem parameters while making no assumption of zero residual circulation. The theory agrees well with a coarse-resolution ocean general circulation model configured in an idealized single-basin domain with a circumpolar channel.

We find that the dynamics of the overturning circulation can be well classified by two limiting dynamical regimes, corresponding to weak and strong diapycnal mixing. The transition between the two regimes is described by nondimensional number ε given generically by (2.21b) and specifically by (2.23) and (2.31) in the weak and strong mixing limits, and this number parameterizes the strength of the diffusion-driven circulation relative to the wind-driven overturning circulation. In the limit of weak diapycnal mixing, typical for the middepth ocean, deep stratification throughout the ocean is produced by the effects of wind and eddies in

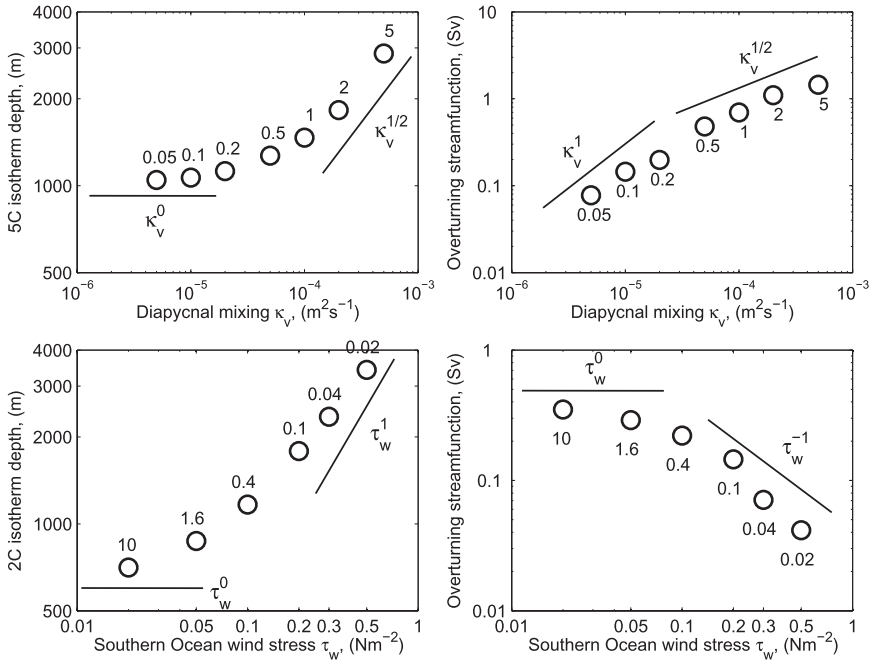

FIG. 13. (left) Depth of the temperature isoline in meters and (right) the rate of the overturning circulation (Sv) as a function of (top) diapycnal diffusivity and (bottom) the Southern Ocean wind stress. Numbers next to markers indicate the value of the nondimensional parameter ε.

a circumpolar channel and maintained even in the limit of vanishing diapycnal diffusivity and in a flat-bottomed ocean. The overturning circulation across the deep stratification is driven by the diapycnal mixing in the basin away from the channel but is sensitive, through changes in stratification, to the wind and eddies in the circumpolar channel. In this limit, the characteristic vertical scale of stratification is independent of diapycnal diffusivity and scales with the wind stress in the channel as τ_w^1. The rate of the overturning circulation is linearly proportional to diapycnal diffusivity κ_v and inversely proportional to the wind stress and therefore as τ_w^{-1}. The dependence of overturning circulation rate on the wind stress is indirect through changes in stratification: stronger wind over the channel stretches stratification from the upper to the deep ocean, decreases its curvature, and thus reduces diffusion-driven overturning circulation.

In the limit of strong diapycnal mixing, which may be of relevance for large-scale numerical models (e.g., Bryan 1991) or the observed abyssal ocean, given the large values of diapycnal diffusivity that are sometimes measured in the abyss (e.g., Polzin et al.1997), deep stratification is primarily set by a combination of eddies in the channel and diapycnal mixing in the basin, with the wind over the circumpolar channel playing a secondary role. In this limit, both the vertical scale of stratification and the rate of the overturning circulation are independent of the wind stress and scale with the diapycnal diffusivity as $\kappa_v^{1/2}$. Weaker dependence of the rate of the overturning circulation on the diapycnal diffusivity in this limit results from the fact the strong diapycnal mixing not only drives the overturning circulation across the deep stratification but also effectively modifies the stratification itself.

b. Discussion

There are a few caveats and shortcomings of this work that we now mention. First, the geometry used is highly idealized and did not include a topographic ridge across the circumpolar channel, as is done sometimes to better represent the geography of the Drake Passage. The presence of the ridge can support geostrophic circulation across the channel that will add to the ageostrophic circulation described in this paper to form the lower cell of the overturning circulation. Although the transport from the channel region to the basin away from the channel can be maintained geostrophically if the ridge is present, the return flow to the surface mixed layer across the channel is above the ridge and hence has to obey the dynamics described here. Thus, the sensitivity of the overturning circulation described here is expected to hold. However, to test this, an extension of the theory or numerical experiments including topographic ridge are needed.

Second, the dynamics of the overturning circulation described here is limited to isopycnals outcropping only in the circumpolar channel: the upper overturning cell, the NADW, is absent in this study and this prevents our work from being a complete theory of subthermocline dynamics. A more complete theory would include the dynamics of both the upper (NADW) and lower (AABW) cells and their interaction. Although, in the singe-basin, zonally averaged framework properties are not exchanged between the cells, the dynamics of the cells might be coupled through changes in stratification. We will present an extension of our work to include these dynamics in the near future.

Finally, the specific parameter dependence of the stratification and the overturning circulation obtained in this studying depends on the choice of the eddy parameterization, and we made perhaps the simplest possible choice by using a diffusive model in an adiabatic framework. We do point out that, although the specific predictions of our theory do depend on this choice, the general structure of the theory does not. The theory could, for example, be recouched using a different type of eddy parameterization. The theory does agree well with the numerical ocean general circulation model that uses similar eddy parameterization; its quantitative agreement with eddy-resolving simulations will be limited by the ability of the eddy parameterization.

Acknowledgments. We thank two anonymous reviewers for their useful comments and suggestions. We acknowledge support from NOAA via Award NA08OAR4320752 and from NSF via Award OCE-1027603.

REFERENCES

Andrews, D. G., and M. E. McIntyre, 1976: Planetary waves in horizontal and vertical shear: The generalized Eliassen-Palm relation and the mean zonal acceleration. *J. Atmos. Sci.,* **33,** 2031–2048.

Bryan, K., 1991: Poleward heat transport in the ocean. A review of a hierarchy of models of increasing resolution. *Tellus,* **43B,** 104–115.

Colin de Verdière, A., 1989: On the interaction of wind and buoyancy driven gyres. *J. Mar. Res.,* **47,** 595–633.

Conkright, M. E., and Coauthors, 2002: *Introduction*. Vol. 1, *World Ocean Database 2001,* NOAA Atlas NESDIS 42, 159 pp.

Eady, E. T., 1957: The general circulation of the atmosphere and oceans. *The Earth and Its Atmosphere,* D. R. Bates, Ed., Basic Books, 130–151.

Ferrari, R., S. M. Griffies, A. J. Nurser, and G. K. Vallis, 2010: A boundary-value problem for the parameterized mesoscale eddy transport. *Ocean Modell.,* **32,** 143–156.

Gent, P. R., and J. C. McWilliams, 1990: Isopycnal mixing in the ocean circulation models. *J. Phys. Oceanogr.,* **20,** 150–155.

Gnanadesikan, A., 1999: A simple predictive model for the structure of the oceanic pycnocline. *Science,* **283,** 2077–2079.

Griffies, S. M., M. J. Harrison, R. C. Pacanowski, and A. Rosati, 2004: A technical guide to MOM4. GFDL Ocean Group Tech. Rep., 337 pp.

Henning, C. C., and G. K. Vallis, 2004: The effects of mesoscale eddies on the main subtropical thermocline. *J. Phys. Oceanogr.,* **34,** 2428–2443.

——, and ——, 2005: The effects of mesoscale eddies on the stratification and transport of an ocean with a circumpolar channel. *J. Phys. Oceanogr.,* **35,** 880–896.

Huang, R. X., 1988: On boundary value problems of the ideal-fluid thermocline. *J. Phys. Oceanogr.,* **18,** 619–641.

Ito, T., and J. Marshall, 2008: Control of lower limb circulation in the southern ocean by diapycnal mixing and mesoscale eddy transfer. *J. Phys. Oceanogr.,* **38,** 2832–2845.

Johnson, G. C., and H. L. Bryden, 1989: On the size of the Antarctic Circumpolar Current. *Deep-Sea Res.,* **36,** 39–53.

Kalnay, E., and Coauthors, 1996: The NCEP/NCAR 40-Year Reanalysis Project. *Bull. Amer. Meteor. Soc.,* **77,** 437–471.

Kamenkovich, I., and P. Goodman, 2000: The dependence of the AABW formation on vertical diffusivity. *Geophys. Res. Lett.,* **27,** 3739–3742.

Killworth, P. D., 1987: A continuously stratified nonlinear ventilated thermocline. *J. Phys. Oceanogr.,* **17,** 1925–1943.

Luyten, J., J. Pedlosky, and H. Stommel, 1983: The ventilated thermocline. *J. Phys. Oceanogr.,* **13,** 292–309.

Marshall, J., and T. Radko, 2003: Residual mean solutions for the Antarctic Circumpolar Current and its associated overturning circulation. *J. Phys. Oceanogr.,* **33,** 2341–2354.

——, and ——, 2006: A model of the upper branch of the meridional overturning of the Southern Ocean. *Prog. Oceanogr.,* **70,** 331–345.

Munk, W. H., 1966: Abyssal recipes. *Deep-Sea Res.,* **13,** 707–730.

——, and C. Wunsch, 1998: Abyssal recipes II: Energetics of tidal and wind mixing. *Deep-Sea Res.,* **45,** 1977–2010.

Pedlosky, J., 1992: The baroclinic structure of the abyssal circulation. *J. Phys. Oceanogr.,* **22,** 652–659.

Polzin, K. L., J. M. Toole, J. R. Ledwell, and R. W. Schmitt, 1997: Spatial variability of turbulent mixing in the abyssal ocean. *Science,* **276,** 93–96.

Radko, T., 2005: Analytical solutions for the ACC and its overturning circulation. *J. Mar. Res.,* **63,** 1041–1055.

Robinson, A. R., and H. Stommel, 1959: The oceanic thermocline and the associated thermocline circulation. *Tellus,* **11,** 295–308.

Salmon, R., 1990: The thermocline as an internal boundary layer. *J. Mar. Res.,* **48,** 437–469.

Samelson, R. M., 1999: Geostrophic circulation in a rectangular basin with a circumpolar connection. *J. Phys. Oceanogr.,* **29,** 3175–3184.

——, 2004: Simple mechanistic models of middepth meridional overturning. *J. Phys. Oceanogr.,* **34,** 2096–2103.

——, 2009: A simple dynamical model of the warm-water branch of the middepth meridional overturning circulation. *J. Phys. Oceanogr.,* **39,** 1216–1230.

——, and G. K. Vallis, 1997: Large-scale circulation with small diapycnal diffusion: The two-thermocline limit. *J. Mar. Res.,* **55,** 223–275.

Stommel, H., and A. B. Arons, 1960: On the abyssal circulation of the World Ocean—I. Stationary planetary flow patterns on a sphere. *Deep-Sea Res.,* **6,** 140–154.

——, and J. Webster, 1963: Some properties of the thermocline equations in a subtropical gyre. *J. Mar. Res.,* **44,** 695–711.

Toggweiler, J. R., and B. Samuels, 1998: On the ocean's large-scale circulation in the limit of no vertical mixing. *J. Phys. Oceanogr.,* **28,** 1832–1852.

Vallis, G. K., 2000: Large-scale circulation and production of stratification: Effects of wind, geometry, and diffusion. *J. Phys. Oceanogr.,* **30,** 933–954.

Welander, P., 1959: An advective model of the ocean thermocline. *Tellus,* **11,** 309–318.

——, 1971: The thermocline problem. *Philos. Trans. Roy. Soc. London,* **270A,** 415–421.

Wolfe, C. L., and P. Cessi, 2010: What sets the mid-depth stratification in eddying ocean model. *J. Phys. Oceanogr.,* **40,** 1520–1538.

Zhao, R., and G. K. Vallis, 2008: Parameterizing mesoscale eddies with residual and Eulerian schemes and a comparison with eddy permitting models. *Ocean Modell.,* **23,** 1–12.